

DOPPLER WIND ANALYSIS OF THE AIRFLOW IN A  
STRATIFORM FRONTAL RAINBAND IN THE PACIFIC NORTHWEST  
USING A BISTATIC RADAR NETWORK

Mark T. Stoelinga\* , John D. Locatelli and Peter V. Hobbs

*University of Washington, Seattle, Washington*

J. Vivekanandan

*National Center for Atmospheric Research, Boulder, Colorado*

## 1. INTRODUCTION

During January and February 2001, a bistatic radar network was deployed along the coast of Washington state during the IMPROVE field project for the purpose of mapping out the three-dimensional air motions within frontally driven precipitation systems in the near-offshore waters. IMPROVE, which stands for Improvement of Microphysical Parameterization through Observational Verification Experiment (Mass 2003; Stoelinga et al. 2003), is a research effort involving field observations, analysis, and numerical modeling, and is aimed at verifying and improving bulk microphysical parameterization schemes used in mesoscale models. During the field studies, remotely sensed and in situ microphysical data were gathered from radar and research aircraft, respectively. In addition, other measurements of standard meteorological variables (wind, pressure, temperature, and humidity) were gathered from a variety of sources, to verify the kinematic and thermodynamic aspects of the model simulations, thus isolating any problems with the microphysical schemes.

A key component of the observational strategy in IMPROVE-1 was the deployment of the National Center for Atmospheric Research (NCAR) Bistatic Network (BINET). The bistatic approach to Doppler velocity measurements (Wurman et al. 1993; Wurman 1994) is a practical and cost-effective alternative to the traditional approach of using multiple, monostatic radars. In the bistatic method, a single transmitting/receiving (monostatic) radar is used, but echoes from the transmitted pulse are also received by several passive receiving (bistatic) antennas at other locations. Bistatic antennas are simpler and cheaper to deploy than multiple monostatic radars. In addition, the bistatic approach offers the advantage of taking simultaneous multi-Doppler measurements of each sampled volume, since all receivers detect echoes from the same transmitted pulse. Several studies have demonstrated success in obtaining wind

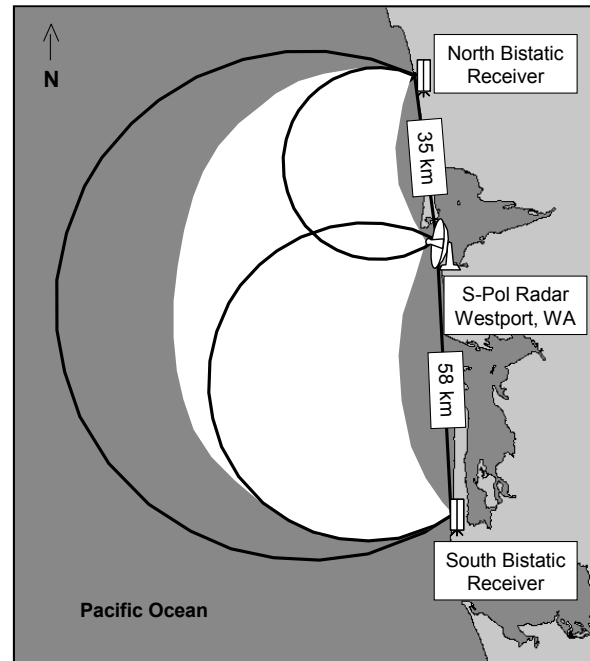


FIG. 1. The bistatic network arrangement in IMPROVE-1. Black curves indicate  $30^\circ$  dual-Doppler lobes for the three receiver pairs. White area indicates region of usable dual-Doppler coverage.

fields from bistatic networks (Wurman 1994; Protat and Zawadzki 1999; Friedrich et al. 2000). This paper discusses the set-up of the IMPROVE-1 bistatic network and the data obtained.

## 2. BINET DEPLOYMENT IN IMPROVE-1

The arrangement of BINET during IMPROVE-1 (Fig. 1) consisted of the NCAR S-band (10.7-cm) Polarimetric ("S-Pol") radar at Westport, Washington, and two bistatic receivers: one north of S-Pol ("North") with a 35-km baseline, and one south of S-Pol ("South") with a 58-km baseline. The differing baselines were chosen due to siting considerations and a desire to test the trade-off between size of coverage area and accuracy of winds retrieved. The  $30^\circ$  Doppler lobes (i.e., regions in which the angle between the two Doppler wind components is at least  $60^\circ$ ) for the three pairs of S-Pol/North, S-Pol/South,

---

\* *Corresponding author address:*  
Mark T. Stoelinga, University of Washington,  
Department of Atmospheric Sciences,  
Box 351640, Seattle, WA, 98126.

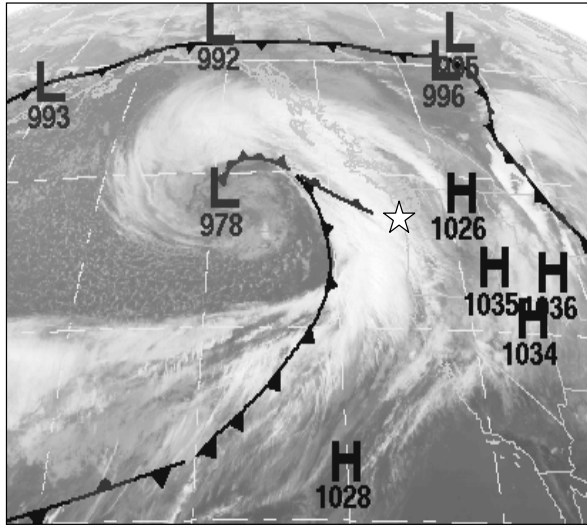


FIG. 2. Infrared satellite image at 0000 UTC 2 Feb 2001. Also shown are frontal positions analyzed by the National Weather Service. White star shows location of bistatic radar network.

and North/South are shown in the figure. Note that these lobes are smaller than the  $30^\circ$  lobes for a conventional Doppler radar configuration of two monostatic radars—in fact, they are the same shape as the conventional  $60^\circ$  lobes. Good coverage would be expected within the  $30^\circ$  lobes of the two pairs involving S-Pol. This coverage is extended by the lobe for the North/South pair, although sensitivity limitations of the bistatic antennas, as well as earth curvature effects, precludes the utility of the long-range portion of the North/South lobe. Based on all of these considerations, the approximate expected area of usable dual-Doppler measurements is shaded in green in Fig. 1.

A challenging aspect of choosing the parameters and scanning strategy for the S-Pol radar in IMPROVE-1 was the variety of roles it played in the field project. As weather systems approached, S-Pol operated with a low PRF ( $600 \text{ s}^{-1}$ ) for long-range weather surveillance. When precipitation features of interest entered the study area, S-Pol served the dual purpose of gathering polarimetric microphysical measurements and dual-Doppler measurements. During these periods,  $180^\circ$  sector volumes (covering the offshore semicircle) were scanned from  $0$  to  $23^\circ$  elevation. Due to the fact that it was impractical to constantly switch between dual-polarization (for microphysical measurements) and vertical-only polarization (which is better for bistatic Doppler measurements), the radar was kept in dual-polarization with as high a PRF as was practical ( $850 \text{ s}^{-1}$ ). Since only the vertically polarized pulses could be used for bistatic measurements, the effective PRF for bistatic measurements was half the actual value, or  $425 \text{ s}^{-1}$ . This led to a low value of the maximum unambiguous (Nyquist) velocity for the bistatic receivers, which made velocity unfolding a

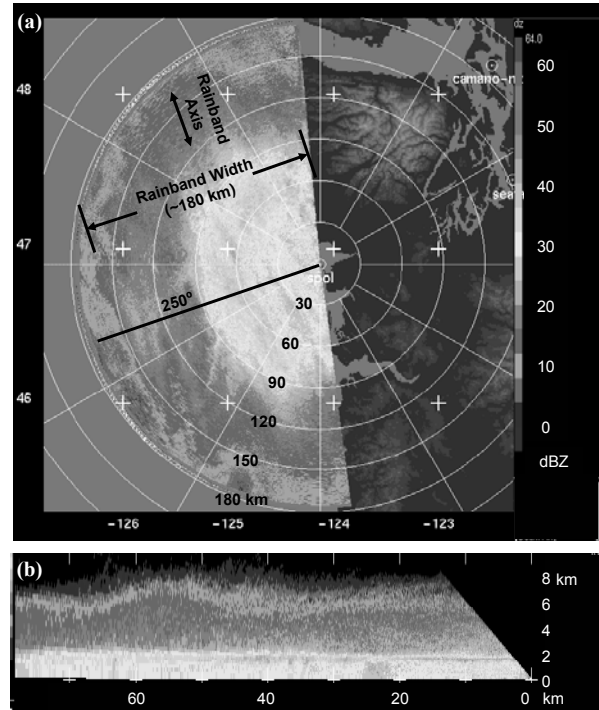


FIG. 3. (a)  $1.5^\circ$ -elevation PPI sector scan from the S-Pol radar at 0218 UTC 2 Feb 2001. (b) RHI scan along the  $250^\circ$  azimuth [shown in (a)] from the S-Pol radar at 0226 UTC 2 Feb 2001.

more challenging problem, as will be discussed further in section 4.

### 3. 1-2 FEBRUARY 2001 RAINBAND

On 1-2 February 2001, an occluding cyclone in the northeast Pacific Ocean brought a vigorous frontal rainband onshore in the Pacific Northwest (Fig. 2). The rainband was associated with an upper cold front that moved ahead of the surface occluded front. A low-elevation scan of reflectivity in the offshore sector from the S-Pol radar (Fig. 3a) showed approximately horizontally uniform precipitation over the entire width of the rainband ( $\sim 180 \text{ km}$ ), with the radar brightband appearing as a ring of enhanced reflectivity at a range of  $70 \text{ km}$ . A RHI scan oriented perpendicular to the band (Fig. 3b) also showed horizontally uniform precipitation, with a distinct brightband just below  $2 \text{ km}$  AMSL, and  $>10 \text{ dBZ}$  reflectivity up to  $7 \text{ km}$  AMSL. This case was chosen as a primary case study for IMPROVE data analysis, and is also a good candidate for bistatic Doppler velocity measurements due to the deep, strong, and widespread radar reflectivity pattern.

### 4. BISTATIC DATA

As previously mentioned, the unfolding of the bistatic Doppler velocity data was somewhat more complicated than for the monostatic Doppler velocity

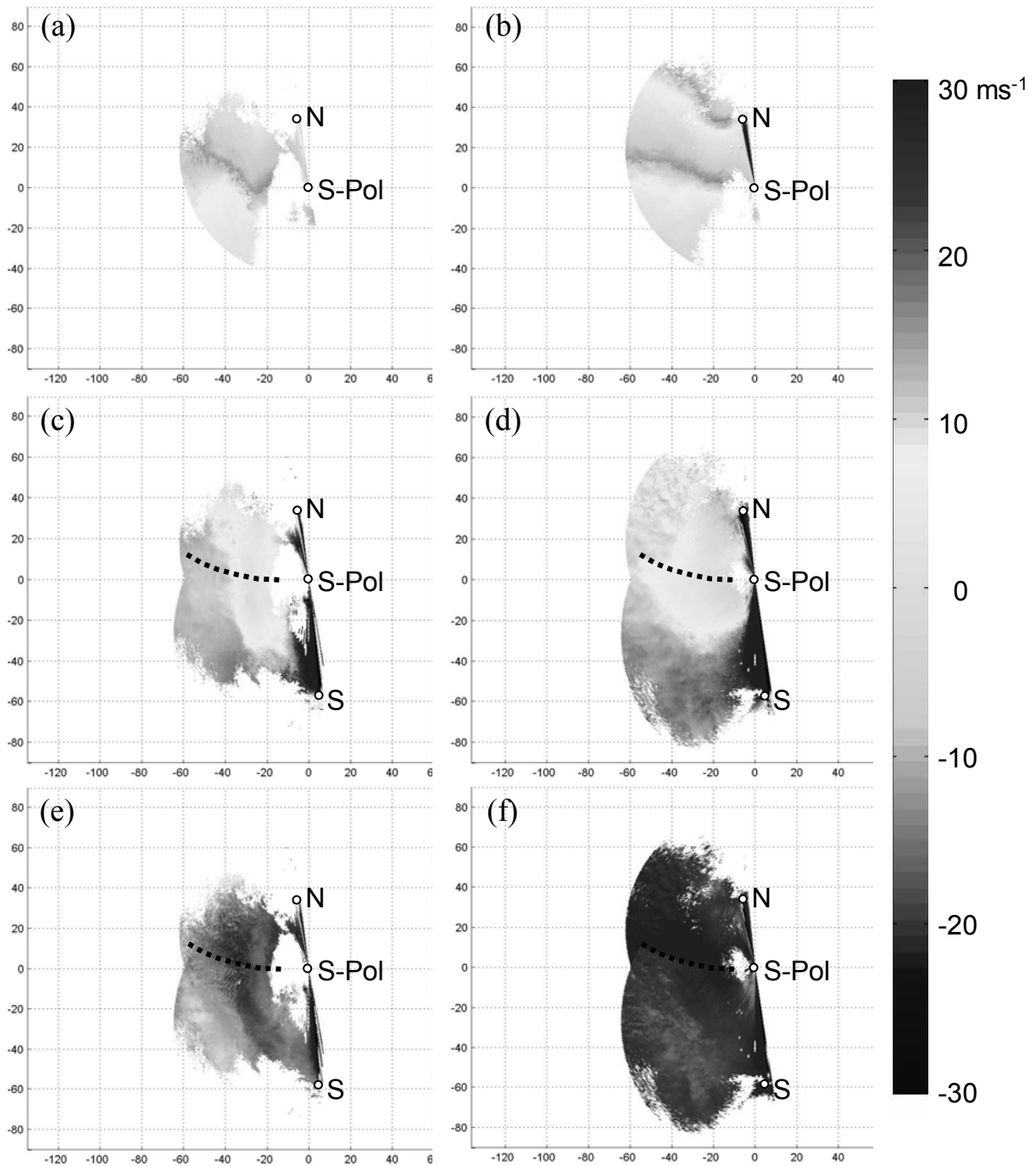


FIG. 4. Bistatic radar data from a  $1.5^\circ$  elevation scan of the S-Pol radar. Left column: 0218 UTC 2 Feb 2001. Right column: 2351 UTC 28 Jan 2001. (a), (b): Doppler radial velocity from the north bistatic receiver. (c), (d): “Best” analysis of the  $u$  component of the wind, using both the S-Pol/North and S-Pol/South dual-Doppler pairs. (e), (f): “Best” analysis of the  $v$  component of the wind, using both the S-Pol/North and S-Pol/South dual-Doppler pairs. “N”, “S-Pol”, and “S” indicate locations of the north bistatic receiver, S-Pol radar, and south bistatic receiver, respectively. Dashed line indicates transition between area where winds are primarily from the S-Pol/North dual-Doppler pair and area where winds are primarily from the S-Pol/South dual-Doppler pair.

data gathered by S-Pol, for two reasons. First, unlike in the monostatic arrangement, the Nyquist velocity is not constant, but includes a dependence on the cosine of half the scattering angle—see Wurman et al. (1993) for a discussion of the bistatic geometry and expansion of the Nyquist velocity. Thus, the unfolding is most easily accomplished for the field of “apparent Doppler velocity” (Protat and Zawadzki 1999), in which the bistatic velocity expansion correction has not been factored in, and the Nyquist velocity is constant. After the unfolding is complete, the velocities are multiplied by the bistatic velocity expansion factor to obtain the true Doppler velocity field. Second, the low effective PRF for vertically polarized pulses resulted in a low Nyquist velocity of 11-15 ms<sup>-1</sup>, so that multiple folds were common in situations of strong wind. While the north bistatic Doppler velocity field in a low-wind test case (28 January 2001, Fig. 4a) displayed only a single fold, the 1-2 February case was characterized by strong southerly winds, resulting in two folds in the north bistatic Doppler velocity field (Fig. 4b) and a total range of nearly 4 $\pi$  in Doppler phase shift. In this case, due to the gradual changes in horizontal wind, it was not difficult to design an algorithm to unfold the data. However, the low effective PRF would likely lead to difficulties in unfolding in situations of strong winds with areas of large, non-uniform horizontal convergence.

As a first approach to constructing 3D wind fields, horizontal wind components were constructed for the S-Pol/North and S-Pol/South Doppler pairs, and were then combined to produce a “best wind” analysis over the entire region of Doppler radar coverage. In regions where the two Doppler pairs both yielded wind vectors, the merging of the two wind fields was based on a combination of weightings for normalized coherent power and bistatic geometry. This “best wind” analysis for the low-wind test case is shown for a 1.5°-elevation PPI scan in Figs. 4c and e. While this method produced seemingly good analyses, with smooth transitions in wind components from the S-Pol/North Doppler region to the S-Pol/South Doppler region, it produced an artificially abrupt transition in both wind components in the high-wind 1-2 February case (Figs. 4d and f). The “best wind” analysis does not include wind vectors constructed from the North/South pair, which would likely improve the quality of the analysis.

However, a preferable approach, which we are in the process of implementing, is that of Protat and Zawadzki (1999), which uses a variational method to construct a 3-D wind field from bistatic dual-Doppler data. It applies weighting functions to the various measurements, as well as to other constraints such as mass continuity. This versatile method can be used in regions of single, dual, and triple Doppler coverage, which lends itself well to the bistatic Doppler arrangement deployed in IMPROVE-1. It can also be used to account for side-lobe contamination, which can be non-negligible for bistatic wind

measurements, even in stratiform precipitation situations (de Elia and Zawadzki 2000).

## 5. SUMMARY

A bistatic radar network consisting of NCAR’s S-Pol radar and two “BINET” receivers was deployed during the IMPROVE-1 field project on the coast of Washington state in January/February 2001. This network provided dual-Doppler measurements in the immediate offshore region of the Washington coast during the passage of primarily stratiform rainbands associated with mid-latitude frontal systems. The data are being used to reconstruct 3-D wind fields for use in verifying the kinematic fields produced by mesoscale model simulations of these rainbands.

## 6. ACKNOWLEDGEMENTS

This research was sponsored by the Mesoscale Dynamic Meteorology and the Physical Meteorology Programs of the Division of Atmospheric Sciences, National Science Foundation, and by the U.S. Weather Research Program. NCAR’s participation in IMPROVE was sponsored by the National Science Foundation and the Federal Aviation Administration.

## 7. REFERENCES

- Protat, A. and I. Zawadzki, 1999: A variational method for real-time retrieval of three-dimensional wind field from multiple-Doppler bistatic radar network data. *J. Atmos. Oceanic Technol.*, **16**, 432–449.
- de Elia, R., and I. Zawadzki, 2000: Sidelobe contamination in bistatic radars. *J. Atmos. Oceanic Technol.*, **17**, 1313-1329.
- Friedrich, K., M. Hagen, and P. Meischner, 2000: Vector wind field determination by bistatic multiple-Doppler radar. *Phys. Chem. Earth (B)*, **25**, 1205-1208.
- Mass, C. F., 2003: The IMPROVE experiment: Goals and program description. *Proc. of 31st Conf. Radar Meteor.*, Seattle, AMS, (this volume).
- Stoelinga, M. T., and co-authors, 2003: Improvement of microphysical parameterization through observational verification experiment (IMPROVE). *Bull. Amer. Meteor. Soc.*, **84**, in press.
- Wurman, J., S. Heckman, and D. Boccippio, 1993: A bistatic multiple-Doppler radar network. *J. Appl. Meteor.*, **32**, 1802-1814.
- \_\_\_\_\_, 1994: Vector winds from a single-transmitter bistatic dual-Doppler radar network. *Bull. Amer. Meteor. Soc.*, **75**, 983-994.